

# Syntheses of $\text{TiO}_2(\text{B})$ nanowires and $\text{TiO}_2$ anatase nanowires by hydrothermal and post-heat treatments

Ryuhei Yoshida, Yoshikazu Suzuki\*, Susumu Yoshikawa\*

*Institute of Advanced Energy, Kyoto University, Uji, Kyoto 611-0011, Japan*

Received 28 February 2005; received in revised form 23 April 2005; accepted 24 April 2005

Available online 23 May 2005

## Abstract

$\text{TiO}_2(\text{B})$  nanowires and  $\text{TiO}_2$  anatase nanowires were synthesized by the hydrothermal processing in 10 M NaOH aq. at 150 °C followed by the post-heat treatment at 300–800 °C. As-synthesized Na-free titanate nanowires (prepared by the hydrothermal treatment and repeated ion exchanging by HCl (aq.)) were transformed into  $\text{TiO}_2(\text{B})$  structure with maintaining 1-D morphology at 300–500 °C, and further transformed into anatase structure at 600–800 °C with keeping 1-D shape. At 900 °C, they transformed into rod-shaped rutile grains. Microstructure of these 1-D  $\text{TiO}_2$  nanomaterials is reported.

© 2005 Elsevier Inc. All rights reserved.

**Keywords:** Hydrothermal process;  $\text{TiO}_2(\text{B})$  nanowire; Anatase nanowire; Microstructure

## 1. Introduction

One-dimensional  $\text{TiO}_2$ -related materials, such as nanotubes, nanowires, and nanofibers have attracted particular interest because of their unique microstructure and promising functions. After the pioneer work on  $\text{TiO}_2$ -related nanotubes preparation by Kasuga et al. [1,2] the hydrothermal method in alkali solution has become one of the most powerful techniques to prepare a wide range of  $\text{TiO}_2$ -related 1-D nanomaterials. In their original work [1,2] single crystal nanotubes (firstly reported as  $\text{TiO}_2$ -anatase) with small diameter of ca. 10 nm were obtained by the hydrothermal treatment of  $\text{TiO}_2$  powder in 10 M NaOH aqueous solution, without using any templates.

Many groups have tried to modify the processing or to analyze the structure of the nanotubes, and have reported that the synthetic mechanism should be the sheet folding [3–5]; the nanotubes are composed of a layered titanate rather than  $\text{TiO}_2$  anatase, that is,

reported as  $\text{H}_2\text{Ti}_3\text{O}_7 \cdot x\text{H}_2\text{O}$  [6–8],  $\text{Na}_x\text{H}_{2-x}\text{Ti}_3\text{O}_7$  [9],  $\text{H}_2\text{Ti}_4\text{O}_9 \cdot \text{H}_2\text{O}$  [10],  $\text{H}_2\text{Ti}_2\text{O}_4(\text{OH})_2$  [11], and so on.

The hydrothermal method has been expanded to prepare other  $\text{TiO}_2$ -related 1-D nanomaterials, such as  $\text{K}_2\text{Ti}_6\text{O}_{13}$  nanowires [12],  $\text{H}_2\text{Ti}_3\text{O}_7$ – $\text{H}_2\text{Ti}_6\text{O}_{13}$  nanofibers [13], and  $\text{TiO}_2(\text{B})$  nanowires [14]. In general, hydrothermal treatment at a slightly higher temperature (~150 °C or higher) or in stronger alkali solution (conc. NaOH(aq.) or KOH(aq.)) results in the formation of solid nanowires (or even long nanofibers) rather than scrolled nanotubes, because the normal unidirectional crystal growth becomes preferential at these conditions. Although the nanotube structure is attractive due to its high surface area, titanate nanotubes with free-alkali ions are usually unstable at high temperatures (at ~500 °C) and convert into anatase particles [8,15,16]. To maintain the 1-D nanostructure at higher temperature (typically at 500–800 °C), the solid nanowire form should be more favorable.

As mentioned above, Armstrong et al. have recently synthesized  $\text{TiO}_2(\text{B})$  nanowires via hydrothermal treatment and post-heat treatment [14].  $\text{TiO}_2(\text{B})$  is a metastable polymorph formed by the dehydration of layered or tunnel-structured hydrogen titanate first

\*Corresponding authors. Fax: +81 774 38 3508.

E-mail addresses: [suzuki@iae.kyoto-u.ac.jp](mailto:suzuki@iae.kyoto-u.ac.jp) (Y. Suzuki),  
[s-yoshi@iae.kyoto-u.ac.jp](mailto:s-yoshi@iae.kyoto-u.ac.jp) (S. Yoshikawa).

synthesized in 1980 [17–20], and also called as monoclinic  $\text{TiO}_2$  [21]. Owing to its low density and tunnel structure,  $\text{TiO}_2(\text{B})$  can be a promising Li intercalation host material [14,22]. Although some properties of hydrothermally synthesized  $\text{TiO}_2(\text{B})$  nanowires have been reported [14,23], further studies are required to put them into actual applications.

In this paper, synthesis of  $\text{TiO}_2(\text{B})$  nanowires by hydrothermal and post-heat treatments will be reported in detail. Furthermore, synthesis of  $\text{TiO}_2$  anatase nanowires by the similar processing (obtained by post-heat treatment at higher temperature) will be also reported. As is reported earlier by Brohan et al.,  $\text{TiO}_2(\text{B})$  transforms into anatase above  $\sim 550^\circ\text{C}$  [24]. Thus, by optimizing the post-heat treatment temperature,  $\text{TiO}_2$  anatase nanowires are successfully obtained.

## 2. Experimental procedure

### 2.1. Synthesis of titanate nanowires by hydrothermal synthesis

A commercial, fine  $\text{TiO}_2$  (anatase) powder (Ishihara Sangyo Ltd., ST-01,  $\sim 300\text{ m}^2/\text{g}$ ) was used as a starting material. A total of 2 g of  $\text{TiO}_2$  powder and 25 mL of 10 M NaOH aqueous solution were put into a Teflon-lined stainless autoclave (the rate of  $\text{TiO}_2$  powder and NaOH aq. is 0.08 g/mL). The autoclave was heated and stirred at  $150^\circ\text{C}$  for 72 h. After it was cooled down to room temperature, it was washed by  $\text{H}_2\text{O}$  and filtered in the vacuum. The obtained precipitation was put into 500 mL of HCl aqueous solution at pH2 and stirred for 24 h. After 24 h, the solution was centrifuged and the precipitation was obtained. This HCl treatment was repeated 3 times in order to remove residual Na ions [16]. After HCl treatment the obtained precipitation was washed by distilled water and dried by freeze dryer. The as-synthesized titanate powder was composed of nanowires with no residual Na ions. The experimental procedure is shown in Fig. 1.

### 2.2. Post-heat treatment of $\text{TiO}_2$ -related nanowires

Titanate nanowires, obtained by the above-mentioned method, were heated in an air atmosphere at  $100\text{--}900^\circ\text{C}$  for 2 h. Crucibles containing as-synthesized nanowires were put into a preheated oven of  $100\text{--}900^\circ\text{C}$ . After 2 h heat-treatment, they were taken out from the oven and cooled down to the room temperature.

### 2.3. Characterization

The microstructures of the as-synthesized and the heat-treated samples were observed by scanning electron microscopy (SEM; JEOL, JSM-6500FE) and

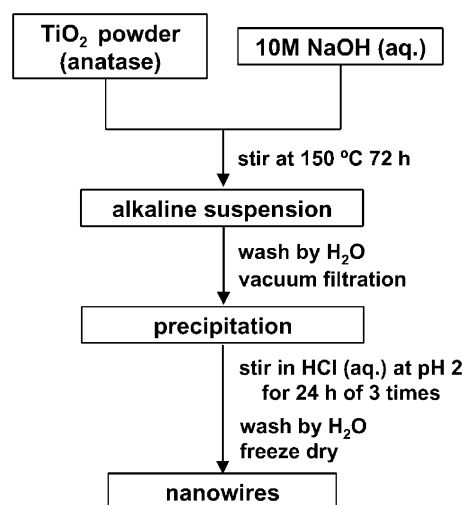


Fig. 1. Schematic representation for experimental procedure.

transmission electron microscopy (TEM; JEOL, JEM-200CX). The powder X-ray diffraction (XRD) patterns of the samples were obtained by Rigaku RINT-2100 diffractometer ( $\text{CuK}\alpha$  radiation, operated at 40 kV and 40 mA). The dehydration and transformation behavior of as-synthesized nanowires was also analyzed by thermogravimetry-differential thermal analysis (TG-DTA; SHIMADZU, DTG-50 H).

## 3. Results and discussion

### 3.1. As-synthesized nanowires

Fig. 2 shows the SEM images, TEM images and nitrogen adsorption isotherms of the samples prepared by hydrothermal method for 72 h at (a–c)  $120^\circ\text{C}$  and (d–f)  $150^\circ\text{C}$ , respectively. Both samples were  $\text{H}_2\text{O}$  washed, acid treated at pH2 for 24 h, 3 times, and then freeze-dried. As described in introduction part, the  $120^\circ\text{C}$ -treated sample was composed of titanate nanotubes and the  $150^\circ\text{C}$ -treated one was composed of titanate nanowires. From the SEM images, both diameter and length of nanowires were larger than those of nanotubes; the diameter and length of nanowires were about 10–50 nm and several  $\mu\text{m}$ , respectively. TEM images and nitrogen adsorption isotherms clearly indicated the difference of nanotubes and nanowires. The  $150^\circ\text{C}$ -treated sample was solid (not hollow) (Fig. 2(e)) and did not contain mesopores (Fig. 2(f)). Although mesopores in nanotubes (Fig. 2(c)) are attractive to obtain a high-surface area material, they destabilize 1-D nanostructure at  $\sim 500^\circ\text{C}$  [16]. The hydrothermal temperature to obtain solid nanowires in our study,  $150^\circ\text{C}$ , was  $20^\circ\text{C}$  lower than Armstrong et al. [14]. This slight difference can be attributable to the use of hot-stirrer during the hydrothermal processing.

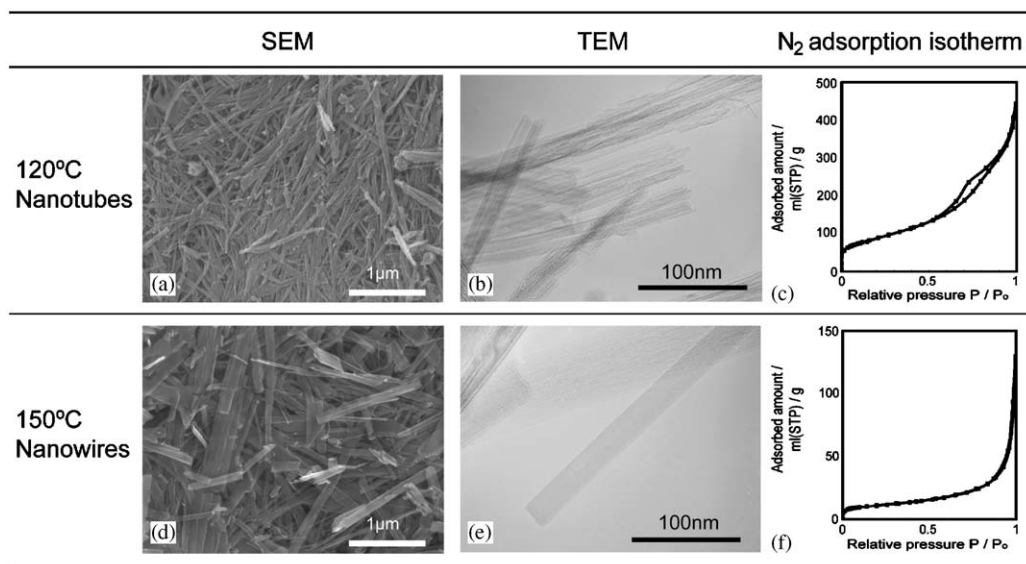


Fig. 2. SEM, TEM images and N<sub>2</sub> adsorption isotherms of the samples prepared by hydrothermal method for 72 h: (a–c) at 120 °C; (d–f) at 150 °C. After the hydrothermal treatment, samples were washed by H<sub>2</sub>O and subsequently HCl treated at pH2 for 3 times, respectively; IUPAC type-IV pattern (indicating the mesopores) was observed in Fig. 2(c) but not in Fig. 2 (f).

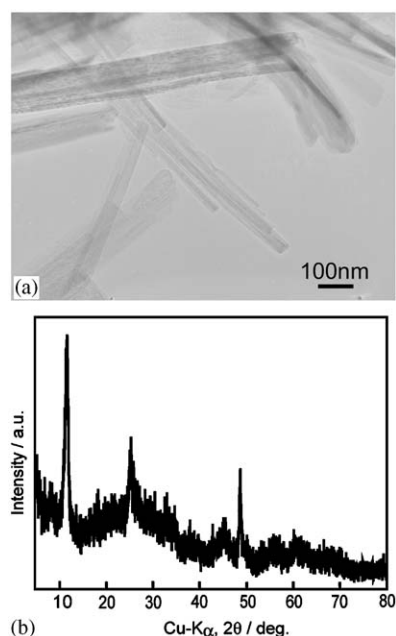


Fig. 3. TEM image and XRD pattern of the titanate nanowires prepared by hydrothermal method at 150 °C for 72 h and H<sub>2</sub>O wash and subsequent HCl treatment pH2 for 3 times.

For the following experiments, titanate nanowires were used as precursor to obtain TiO<sub>2</sub>(B) and TiO<sub>2</sub> anatase nanowires. Fig. 3 shows a TEM image and an XRD pattern of the titanate nanowires, prepared by the hydrothermal method at 150 °C at 72 h. The diameter of each titanate nanowire was 10–50 nm, and some nanowires formed bundles of ~100 nm in diameter. The XRD pattern resembled that in Ref. [14], indicating layered or tunnel-structured titanate structure, H<sub>2</sub>Ti<sub>n</sub>

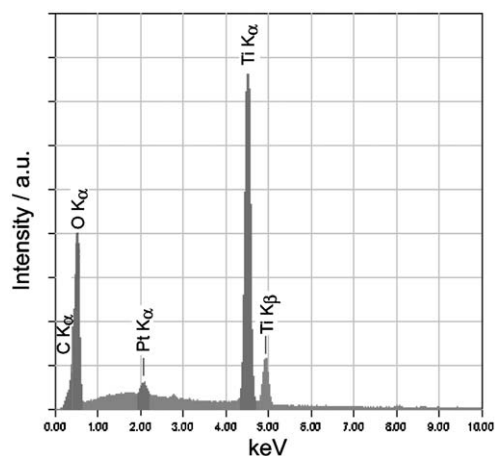


Fig. 4. EDS spectrum of the TiO<sub>2</sub>-related nanowires prepared by hydrothermal method at 150 °C for 72 h and H<sub>2</sub>O wash and subsequent HCl treatment pH2 for 3 times. Pt peaks are arisen from the coating for SEM observation and sample stages.

O<sub>2n+1</sub> · xH<sub>2</sub>O. Further electron diffraction study will be needed to clarify the as-synthesized nanowires.

As described in our previous work [16], Na concentration in the NaOH-treated samples can be minimized by repeated ion-exchanging treatment by HCl. Fig. 4 shows an EDS spectrum of the nanowires. Na concentration in the sample was less than the EDS lower limit of detection.

### 3.2. Nanowires with post-heat treatment (100–500 °C)

Figs. 5 and 6 show the SEM images and XRD patterns of the as-synthesized titanate nanowires and the heat-treated samples: (a) is the as-synthesized nanowires

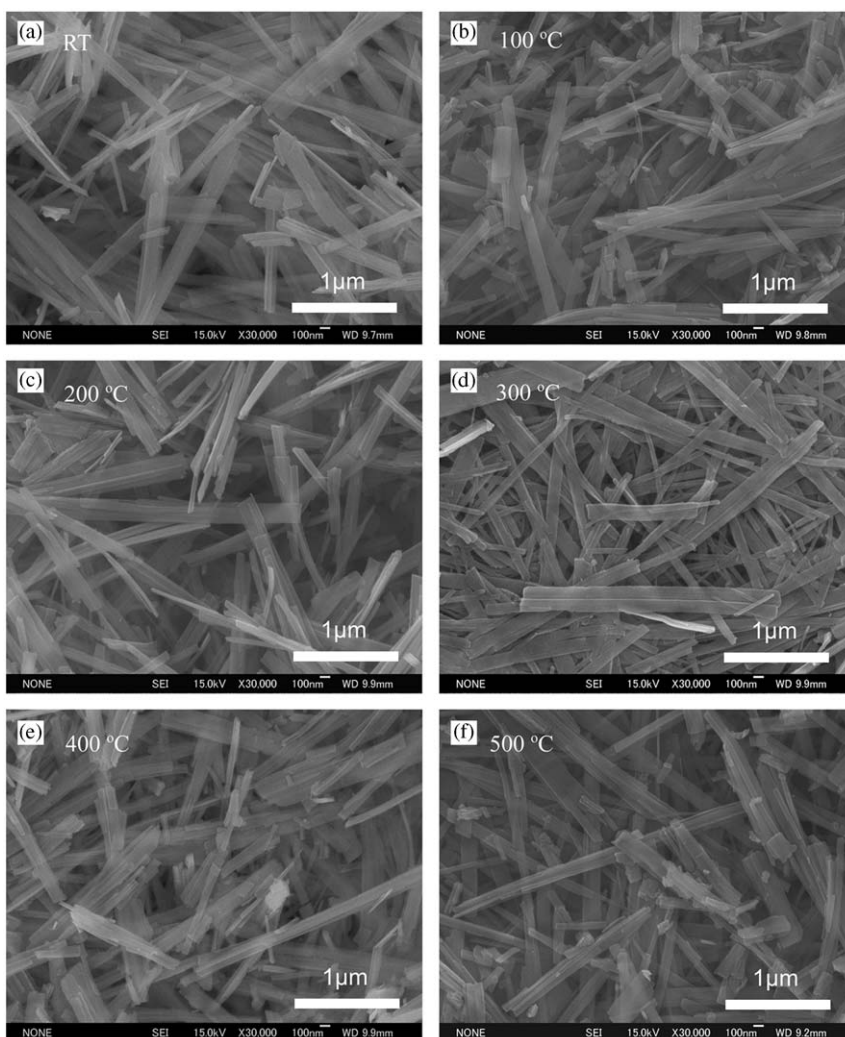


Fig. 5. SEM images of  $\text{TiO}_2$ -related nanowires (prepared for 72 h at  $150^\circ\text{C}$ ), (a) as-synthesized, and calcined for 2 h; (b) at  $100^\circ\text{C}$ ; (c) at  $200^\circ\text{C}$ ; (d) at  $300^\circ\text{C}$ ; (e) at  $400^\circ\text{C}$ ; (f) at  $500^\circ\text{C}$ .

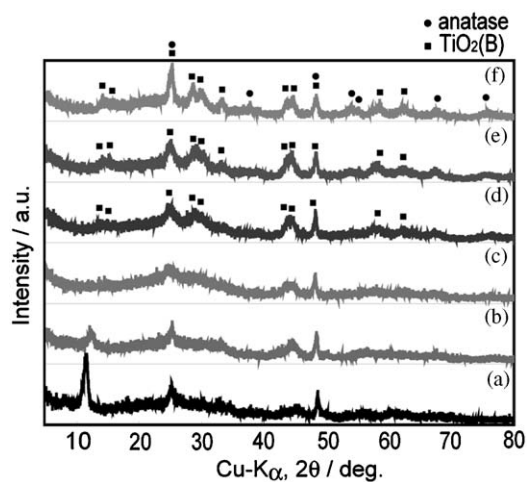


Fig. 6. XRD patterns of  $\text{TiO}_2$ -related nanowires (prepared for 72 h at  $150^\circ\text{C}$ ), (a) as-synthesized, and calcined for 2 h; (b) at  $100^\circ\text{C}$ ; (c) at  $200^\circ\text{C}$ ; (d) at  $300^\circ\text{C}$ ; (e) at  $400^\circ\text{C}$ ; (f) at  $500^\circ\text{C}$ .

(hydrothermally synthesized at  $150^\circ\text{C}$  for 72 h, and ion-exchanged by repeated acid treatment), and (b)–(f) are samples heated for 2 h at  $100$ ,  $200$ ,  $300$ ,  $400$  and  $500^\circ\text{C}$ , respectively. Apparently, the SEM images of heat-treated samples are almost identical to that of the as-synthesized nanowires. The samples of (a)–(f) are composed of almost only nanowires.

In the XRD patterns of (a) and (b), drastic change was not observed. However, the reflection peak at  $2\theta \sim 10^\circ$  shifts to higher angle and becomes broader. This reflection peak corresponds to the interlayer (or tunnel–tunnel) spacing of titanate. Thus, this peak shift means the decrease of the interlayer spacing. This can be explained by dehydration of  $\text{H}_2\text{O}$  molecules [13,15], contained in the as-synthesized nanowires. The  $300^\circ\text{C}$ -calcined sample had very broad XRD pattern (Fig. 6(c)). At around  $300^\circ\text{C}$ , phase transformation from titanate to  $\text{TiO}_2(\text{B})$  seems to proceed. The XRD patterns



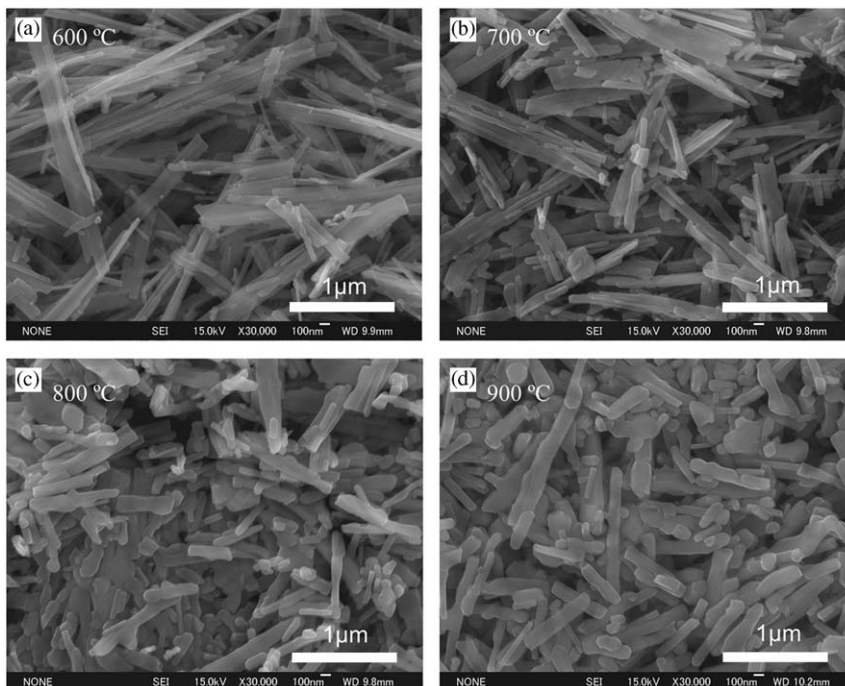


Fig. 7. SEM images of  $\text{TiO}_2$ -related nanowires (prepared for 72 h at  $150^\circ\text{C}$ ) calcined for 2 h (a) at  $600^\circ\text{C}$ ; (b) at  $700^\circ\text{C}$ ; (c) at  $800^\circ\text{C}$ ; (d) at  $900^\circ\text{C}$ .

of (d)–(f) can be indexed as  $\text{TiO}_2(\text{B})$ . In our conditions,  $\text{TiO}_2(\text{B})$  nanowires were synthesized by heat treatment of titanate nanowires at  $300$ – $500^\circ\text{C}$  for 2 h. Recent reports on the synthesis of  $\text{TiO}_2(\text{B})$  nanowires showed similar formation temperature range of  $300$ – $600^\circ\text{C}$  [14] or at  $400$ – $600^\circ\text{C}$  [25]. Some differences can be attributed to the synthesis conditions of precursor nanowires, and kinetics effect (Note that  $\text{TiO}_2(\text{B})$  is a metastable phase).

### 3.3. Nanowires with post-heat treatment ( $600$ – $900^\circ\text{C}$ )

Figs. 7 and 8 show the SEM images and XRD patterns of the heat-treated samples: (a)–(d) are samples heated for 2 h at  $600$ ,  $700$ ,  $800$  and  $900^\circ\text{C}$ , respectively. The SEM images of (a) and (b) show almost only nanowires. Those of (c) and (d) show both nanowires and small amount of particles. Over  $800^\circ\text{C}$ , the surfaces of nanowires became smooth because of the progress of surface diffusion. (At  $>800^\circ\text{C}$ , they may be preferably called as “submicron wires” due to the size enlargement.) The XRD patterns of (a)–(c) are indexed as  $\text{TiO}_2$  anatase phase. The diffraction peaks of (a)–(c) became very sharp, indicating high crystallinity. In the XRD pattern of (d), the formation of  $\text{TiO}_2$  rutile phase is confirmed. Thus, the nanowires transform from  $\text{TiO}_2(\text{B})$  to anatase at  $\sim 600^\circ\text{C}$  and to rutile at  $\sim 900^\circ\text{C}$ .

Generally, anatase phase of  $\text{TiO}_2$  becomes unstable and transforms into rutile phase at the temperature higher than  $700^\circ\text{C}$ . However, the anatase nanowires, prepared by this work, were stable at even  $800^\circ\text{C}$ . So,

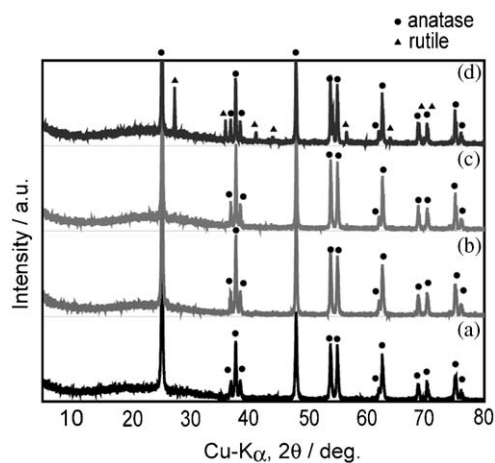


Fig. 8. XRD patterns of  $\text{TiO}_2$ -related nanowires (prepared for 72 h at  $150^\circ\text{C}$ ) calcined for 2 h (a) at  $600^\circ\text{C}$ ; (b) at  $700^\circ\text{C}$ ; (c) at  $800^\circ\text{C}$ ; (d) at  $900^\circ\text{C}$ .

the anatase nanowires might have an advantage for high temperature applications of anatase phase.

### 3.4. TG-DTA analysis

Fig. 9 shows the TG-DTA diagrams for as-synthesized nanowires. The endothermic peak at  $140^\circ\text{C}$  and weight loss correspond to the dehydration of interlayer (or inside tunnel) water and the start of phase transformation from a titanate to  $\text{TiO}_2(\text{B})$ . The exothermic peaks at  $530$  and  $760^\circ\text{C}$  can be attributable to the phase transformation from  $\text{TiO}_2(\text{B})$  to anatase

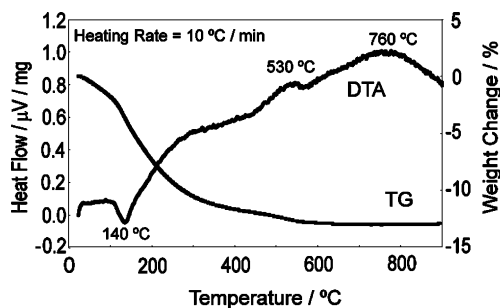


Fig. 9. TG-DTA diagrams for  $\text{TiO}_2$ -related nanowires.

and that from anatase to rutile, respectively. The results of the TG-DTA curves are in good agreement with that of XRD patterns.

### 3.5. TEM observation of a nanowire

A TEM image of a nanowire (obtained by the calcination at  $700\text{ }^\circ\text{C}$  for 2 h) and its enlargement are given in Fig. 10(a) and (b), respectively. The diameter of the nanowire was about 50 nm, and faceted surface was observed (Fig. 10(a)). By a high-resolution image (Fig. 10(b)), two lattice fringes (5.0 and 3.6 Å) were observed. The lattice fringe with 5.0 Å was parallel to the nanowire surface, and the angle between two fringes was  $110^\circ$ .

In an early study by Brohan et al. [24], the transformation from  $\text{TiO}_2(\text{B})$  to anatase was explained by the shear of  $(\bar{2}01)_{\text{TiO}_2(\text{B})}$  plane to form  $(10\bar{3})_{\text{anatase}}$  plane, along with the  $[20\bar{3}]_{\text{TiO}_2(\text{B})}$  direction. The lattice spacings of  $(\bar{2}01)_{\text{TiO}_2(\text{B})}$  and  $(10\bar{3})_{\text{anatase}}$  are 5.08 and 2.43 Å (almost half of the former), respectively [26,27]. In addition, those of  $(110)_{\text{TiO}_2(\text{B})}$  and corresponding  $(101)_{\text{anatase}}$  are 3.57 and 3.52 Å, respectively. Considering these data, the observed nanowire in Fig. 10 can be attributed to a remnant  $\text{TiO}_2(\text{B})$  nanowire at  $700\text{ }^\circ\text{C}$ , with the indication of transforming into anatase phase (see the surface steps, implying the possible shear into anatase phase). Observed angle of  $110^\circ$  was then well-explained by the  $(\bar{2}01)_{\text{TiO}_2(\text{B})}$  and  $(110)_{\text{TiO}_2(\text{B})}$  plane, which can be calculated using the following equation for monoclinic system:

$$\phi = \cos^{-1} \left[ \frac{d_1 d_2}{\sin^2 \beta} \left( \frac{h_1 h_2}{a^2} + \frac{k_1 k_2 \sin^2 \beta}{b^2} + \frac{l_1 l_2}{c^2} - \frac{(l_1 h_2 + l_2 h_1) \cos \beta}{ac} \right) \right],$$

where each character has its usual crystallographic meaning.

### 3.6. Possible applications of nanowires

As is very recently reported,  $\text{TiO}_2(\text{B})$  nanowire is a promising Li-storage material [14,28], which can be

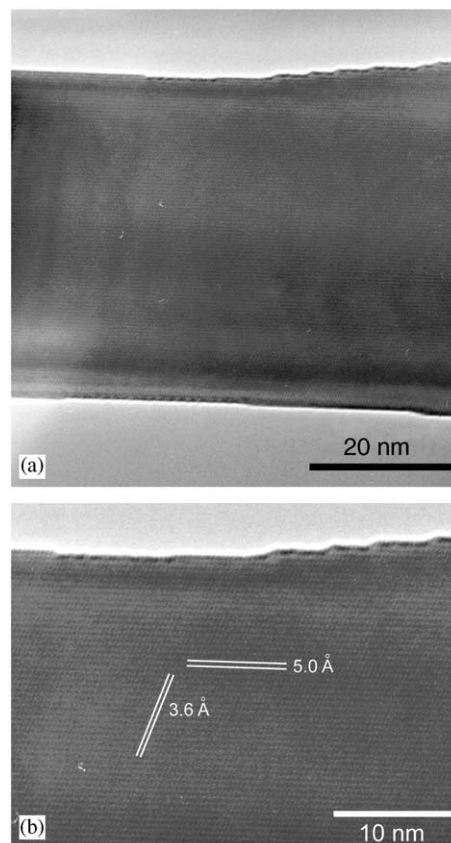


Fig. 10. TEM micrographs of (a) a  $\text{TiO}_2$  nanowire (obtained by the calcination at  $700\text{ }^\circ\text{C}$  for 2 h) and (b) its enlargement.

expected from the earlier reports on the  $\text{TiO}_2(\text{B})$  phase [17,22]. Other possible applications of  $\text{TiO}_2(\text{B})$  nanowires are photocatalysts and dye-sensitized solar cells (DSC). Since the currently prepared  $\text{TiO}_2(\text{B})$  nanowires (with typical surface area of  $20\text{ m}^2/\text{g}$ ) did not have sufficient surface area for these purposes, our preliminary results were not satisfactory: (e.g., DSC solar energy conversion efficiency using  $\text{TiO}_2(\text{B})$  nanowires was only 0.57% [23]) Decreasing the size of nanowires (like in a very recent paper [29]) is an effective strategy to improve various properties.

## 4. Conclusions

Na-free titanate nanowires were prepared by the hydrothermal synthesis of  $150\text{ }^\circ\text{C}$  for 72 h and repeated HCl treatment. The apparent 1-D morphology of  $\text{TiO}_2$ -related nanowires was thermally stable at any post-heat treatment temperature in this study. At about  $300\text{ }^\circ\text{C}$ , they began to change into  $\text{TiO}_2(\text{B})$  nanowires, and at about  $600\text{ }^\circ\text{C}$ , transformed into anatase-type  $\text{TiO}_2$  nanowires. At higher temperature than  $900\text{ }^\circ\text{C}$ , they began to change into rutile-type  $\text{TiO}_2$  rod-like grains.

## Acknowledgments

A part of this work has been supported by 21COE program “Establishment of COE on Sustainable Energy System” and “Nanotechnology Support Project” of the Ministry of Education, Culture, Sports, Science and Technology (MEXT), Japan.

## References

- [1] T. Kasuga, M. Hiramatsu, A. Hoson, T. Sekino, K. Niihara, *Langmuir* 14 (1998) 3160–3163.
- [2] T. Kasuga, M. Hiramatsu, A. Hoson, T. Sekino, K. Niihara, *Adv. Mater.* 11 (1999) 1307–1311.
- [3] Y.Q. Wang, G.Q. Hu, X.F. Duan, H.L. Sun, Q.K. Xue, *Chem. Phys. Lett.* 365 (2002) 427–431.
- [4] Q. Chen, G.H. Du, S. Zhang, L.M. Peng, *Acta Crystallogr. B* 58 (2002) 587–593.
- [5] Y.F. Chen, C.Y. Lee, M.Y. Yeng, H.T. Chiu, *Mater. Chem. Phys.* 81 (2003) 39–44.
- [6] G.H. Du, Q. Chen, R.C. Che, Z.Y. Yuan, L.-M. Peng, *Appl. Phys. Lett.* 79 (2001) 3702–3704.
- [7] Q. Chen, W.Z. Zhou, G.H. Du, L.-M. Peng, *Adv. Mater.* 14 (2002) 1208–1211.
- [8] Y. Suzuki, S. Yoshikawa, *J. Mater. Res.* 19 (2004) 982–985.
- [9] X. Sun, Y. Li, *Chem. Euro. J.* 9 (2003) 2229–2238.
- [10] A. Nakahira, W. Kato, M. Tamai, T. Isshiki, K. Nishio, H. Aritani, *J. Mater. Sci.* 39 (2004) 4239–4245.
- [11] M. Zhang, Z.S. Jin, J.W. Zhang, X.Y. Guo, J.J. Yang, W. Li, X.D. Wang, Z.J. Zhang, *J. Molec. Catal. A: Chem.* 217 (2004) 203–210.
- [12] G.H. Du, Q. Chen, P.D. Han, Y. Yu, L.M. Peng, *Phys. Rev. B* 67 (2003) 035323.
- [13] Y. Suzuki, S. Pavasupree, S. Yoshikawa, R. Kawahata, *J. Mater. Res.* 20 (2005) 1063–1070.
- [14] A.R. Armstrong, G. Armstrong, J. Canales, P.G. Bruce, *Angew. Chem. Int. Ed.* 43 (2004) 2286–2288.
- [15] R. Yoshida, Y. Suzuki, S. Yoshikawa, *Mater. Chem. Phys.* 91 (2005) 409–416.
- [16] R. Yoshida, Y. Suzuki, S. Yoshikawa, *Mater. Chem. Phys.*, in contribution.
- [17] R. Marchand, L. Brohan, M. Tournoux, *Mater. Res. Bull.* 15 (1980) 1129–1133.
- [18] M. Tournoux, R. Marchand, L. Brohan, *Prog. Solid State Chem.* 17 (1986) 33–52.
- [19] T.P. Feist, S.J. MocarSKI, P.K. Davies, A.J. Jacobson, J.T. Lewandowski, *Solid State Ionics* 28–30 (1988) 1338–1343.
- [20] T.P. Feist, P.K. Davies, *J. Solid State Chem.* 101 (1992) 275–295.
- [21] S. Yin, Y. Fujishiro, J. Wu, M. Aki and, T. Sato, *J. Mater. Proc. Tech.* 137 (2003) 45–48.
- [22] G. Nuspl, K. Yoshikawa, T. Yamabe, *J. Mater. Chem.* 7 (1997) 2529–2536.
- [23] R. Yoshida, Master Thesis, Graduate School of Energy Science, Kyoto University, February 2005.
- [24] L. Brohan, A. Verbaere, M. Tournoux, *Mater. Res. Bull.* 17 (1982) 355–361 (in French).
- [25] Z.-Y. Yuan, B.-Y. Su, *Colloids Surfaces A* 241 (2004) 173–183.
- [26] ICDD-JCPDS database, #46-1238 (TiO<sub>2</sub>(B)).
- [27] ICDD-JCPDS database, #21-1272 (anatase TiO<sub>2</sub>).
- [28] M. Zúkalová, M. Kalbá, L. Kavan, I. Exnar, M. Grätzel, *Chem. Mater.* 17 (2005) 1248–1255.
- [29] X.P. Gao, H.Y. Zhu, G.L. Pan, S.H. Ye, Y. Lan, F. Wu, D.Y. Song, *J. Phys. Chem. B* 108 (2004) 2869–2872.